www.nature.com/hdy

the geneticssociety

ARTICLE

Predicting recombination suppression outside chromosomal inversions in *Drosophila melanogaster* using crossover interference theory

Spencer A. Koury [1,2]✉

Recombination suppression in chromosomal inversion heterozygotes is a well-known but poorly understood phenomenon. Surprisingly, recombination suppression extends far outside of inverted regions where there are no intrinsic barriers to normal chromosome pairing, synapsis, double-strand break formation, or recovery of crossover products. The interference hypothesis of recombination suppression proposes heterozygous inversion breakpoints possess chiasma-like properties such that recombination suppression extends from these breakpoints in a process analogous to crossover interference. This hypothesis is qualitatively consistent with chromosome-wide patterns of recombination suppression extending to both inverted and uninverted regions of the chromosome. The present study generated quantitative predictions for this hypothesis using a probabilistic model of crossover interference with gamma-distributed inter-event distances. These predictions were then tested with experimental genetic data (>40,000 meioses) on crossing-over in intervals that are external and adjacent to four common inversions of *Drosophila melanogaster*. The crossover interference model accurately predicted the partially suppressed recombination rates in euchromatic intervals outside inverted regions. Furthermore, assuming interference does not extend across centromeres dramatically improved model fit and partially accounted for excess recombination observed in pericentromeric intervals. Finally, inversions with breakpoints closest to the centromere had the greatest excess of recombination in pericentromeric intervals, an observation that is consistent with negative crossover interference previously documented near *Drosophila melanogaster* centromeres. In conclusion, the experimental data support the interference hypothesis of recombination suppression, validate a mathematical framework for integrating distance-dependent effects of structural heterozygosity on crossover distribution, and highlight the need for improved modeling of crossover interference in pericentromeric regions.

Heredity (2023) 130:196–208; https://doi.org/10.1038/s41437-023-00593-x

INTRODUCTION

Crossing-over is a fundamental meiotic process that facilitates both correct segregation of chromosomes and reciprocal exchange of genetic material between homologs. Chromosomal inversions were first discovered in *Drosophila melanogaster* by their heterozygous effect as strong crossover suppressors (Muller 1916; Sturtevant 1917, 1921). Given the central importance of crossing-over in both cellular biology and genome science, there is a long-standing interest in how structural features of chromosomes (centromeres, telomeres, rearrangements, etc.) alter the distribution of crossover events along the chromosome axis.

Among the most enigmatic effects of inversion heterozygosity is recombination suppression occurring *outside* of the inverted region. In Diptera, a well-known mechanism for recombination suppression *inside* heterozygous inversions is single crossover events forming acentric and dicentric chromatids that are then selectively excluded from the functional egg (Sturtevant and Beadle 1936; Carson 1946). However, recombination experiments with heterozygous *In(1)dl-49* in *D. melanogaster* (the only instance where single crossover rates both inside and outside the inverted region have been empirically determined) reveal that this acentric/dicentric mechanism causes only one-fourth of the recombination suppression observed inside inverted regions and absolutely none of the recombination suppression observed outside of inversions (Novitski and Braver 1954). Therefore, the acentric/dicentric mechanism accounts for only 16% of the total chromosome-wide suppression phenotype (Stone and Thomas 1935; Sturtevant and Beadle 1936; Novitski and Braver 1954). The present study investigates the hypothesis that this breakdown of the total chromosome-wide suppression phenotype is caused by heterozygous inversion breakpoints inducing crossover interference (Gong et al. 2005). The mathematical development of the interference hypothesis presented here has the potential to account for the remaining 84% of unexplained chromosome-wide recombination suppression phenotype and provides a modeling framework to predict recombination suppression for any interval in heterozygotes of any chromosomal inversion.

In chromosomal regions immediately adjacent to heterozygous inversion breakpoints (up to 3 Mb in Drosophila) crossing-over has not been experimentally observed and was historically assumed to

[1]Department of Ecology and Evolution, Stony Brook University, 650 Life Sciences Building, Stony Brook, NY 11794, USA. [2]Present address: 2613 Ashwood Ave, Nashville, TN 37212, USA. Associate editor: Aurora Ruiz-Herrera. ✉email: spencerkoury@gmail.com

Received: 3 October 2022 Revised: 20 January 2023 Accepted: 20 January 2023
Published online: 1 February 2023

be due to failed synapsis (Dobzhansky 1931; Stone and Thomas 1935; Sturtevant and Beadle 1936; Novitski and Braver 1954; Roberts 1962; Stevison et al. 2011; Miller et al. 2016, 2018; Crown et al. 2018). Further out from breakpoints there are no apparent barriers to normal pairing, synapsis, double-strand break formation, or crossover maturation; and although recombination can occur in these regions, the overall rates of recombination are nonetheless reduced up to 12 Mb outside the inversion (Sturtevant and Beadle 1936; Grell 1962; Roberts 1962). In more distant regions (greater than 13 Mb from breakpoints), recombination rates are slightly elevated and sometimes even exceed standard genetic map expectations. This elevation has been observed on the inverted arm of acrocentric chromosomes (Grell 1962; Roberts 1962) and across the centromere to the uninverted arms of metacentric chromosomes, where it is called the intrachromosomal effect (Dobzhansky and Sturtevant 1931; Dobzhansky 1933; Ramel 1968). Similar increases in recombination rates due to inversion heterozygoisty have been observed on non-homologous chromosomes, in what is known as the interchromosomal effect (Schultz and Redfield 1951; Roberts 1962; Lucchesi and Suzuki 1968; Crown et al. 2018).

The mechanisms for and transitions between the complete, partial, and negative recombination suppression in uninverted regions of inversion heterozygotes are not well-characterized. Furthermore, the general phenomena of heterozygous inversions as modifiers of the genome-wide crossover distribution through the intrachromosomal and interchromosomal effects are well-documented, but not mechanistically understood. Clearly, recombination suppression is a complex phenotype resulting from several types of crossover modification varying in magnitude and depending on the distance from heterozygous inversion breakpoints.

Both the local recombination suppression and genome-wide redistribution of crossing-over in inversion heterozygotes were first described in the pre-molecular era of biology, and more recent analyses of multiply inverted chromosomes of *D. melanogaster* have shown older assumptions about absence of pairing, synapsis, and double-strand break formation near inversion breakpoints to be incorrect (Gong et al. 2005; Miller et al. 2016a; Miller et al. 2016b). To explain the strong suppression of recombination without correspondingly strong defects in the requirements for crossover initiation, Gong et al. (2005) hypothesized heterozygous inversion breakpoints act like chiasmata by altering local synaptonemal complex structure and, thereby, inducing a process analogous to crossover interference. The synaptonemal complex is a dynamic tripartite proteinaceous structure that forms between homologous chromosomes in prophase of meiosis I and facilitates the maturation of double-strand breaks into crossover events in *D. melanogaster* (reviewed in Page and Hawley 2004; Hughes et al. 2018). Analysis of genetic variants that alter spatial distribution of recombination implicates a fundamental role for the synaptonemal complex in crossover interference (Zhang et al. 2014a; Brand et al. 2015; Hatkevich et al. 2017; Capilla-Pérez et al. 2021; France et al. 2021). Thus, the interference hypothesis of recombination suppression is qualitatively consistent with cytological observations, a proposed cytogenetic mechanism, and the statistical pattern of crossover redistribution observed in inversion heterozygotes. Placing the interference hypothesis in a rigorous mathematical framework has the potential to unify the disparate regional effects of inversion heterozygosity under a single mechanism that can be formally tested with quantitative predictions derived from explicit models of crossover interference.

Statistically, crossover interference is defined as spatial non-independence of two crossover events and can be quantified with a coefficient of coincidence (Sturtevant 1913, 1915; Muller 1916; Weinstein 1918). The coefficient of coincidence is a unitless measure expressed as the ratio of observed to expected double

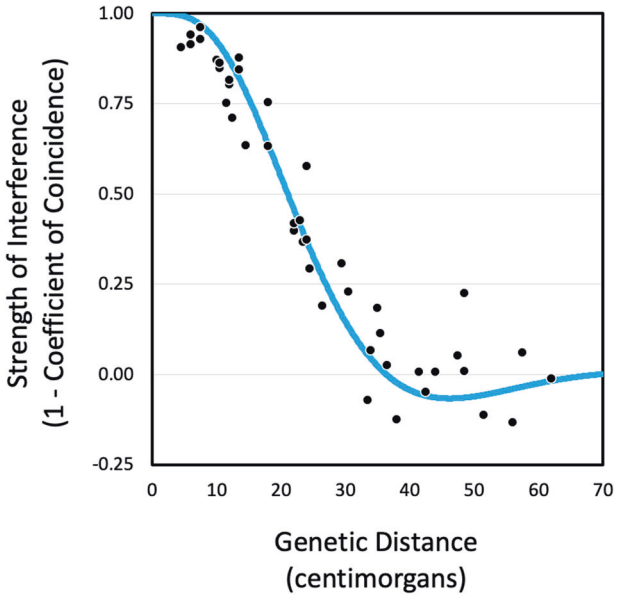

Fig. 1 Decay-with-distance of crossover interference. Black dots represent the strength of interference (1—coefficient of coincidence) plotted by genetic distance between of two crossover events measured in centimorgans (cM) of the *D. melanogaster* genetic map. On this scale, 1.00 indicates absolute crossover interference while 0.00 represents independence of crossover events and, therefore, negative strength of interference indicates a greater than expected rate of double crossovers. Data are from multi-locus recombination experiments on *D. melanogaster X* chromosomes (Morgan et al. 1935; Weinstein 1936). Blue function represents the renewal process model of crossover interference with inter-event distances measured in cM following a gamma distribution fitted by maximum likelihood (McPeek and Speed 1995; Zhao et al. 1995).

crossover events assuming crossover independence, it equals unity in absence of interference, and it is the complement of the strength of crossover interference (Stevens 1936; Bailey 1961). Early development of crossover interference theory was based on data from *D. melanogaster*, where crossover interference was first described (Sturtevant 1915; Muller 1916; Weinstein 1918; Haldane 1919; Stevens 1936; Kosambi 1943; Bailey 1961). Modeling the underlying process for the gold-standard, multi-locus datasets (Morgan et al. 1935; Weinstein 1936), multiple groups arrived at the same conclusion: crossover interference in *D. melanogaster* is most accurately modeled as a renewal process where inter-event distances follow a gamma distribution (Payne 1956; Cobbs 1978; Risch and Lange 1983; Foss et al. 1993; McPeek and Speed 1995; Zhao et al. 1995; Copenhaver et al. 2002). The defining feature of this model is that strength of crossover interference decays with increasing genetic distance measured in centimorgans (cM), a property readily visible in datasets from classic recombination experiments (Fig. 1).

In the context of *D. melanogaster* inversion heterozygosity, the decay-with-distance model suggests: 1) negligible recombination (<0.0001 crossovers per meiosis) will occur within 5 map units of inversion breakpoints, 2) recombination suppression will decay to wildtype rates over approximately 35 map units outside of inversions, and 3) relatively weak elevation of recombination above wildtype rates will be observed in regions 40–60 map units distant from the inverted region (map units refer to genetic distance measured in cM along the standard genetic map of *D. melanogaster*). The apparent negative suppression occurring in regions greater than 40 map units from inversions is analogous to negative inference (Fig. 1) and is a product of damped oscillation as the decay-with-distance function approaches the limit of wildtype recombination levels (Owen 1949; Stam 1979;

McPeek and Speed 1995; Zhao et al. 1995). These three general predictions are qualitatively consistent with the suppression effects classically observed outside of heterozygous inversions (Sturtevant and Beadle 1936; Grell 1962; Miller et al. 2016b).

More precise quantitative predictions for the magnitude and spatial extent of recombination suppression as it decays outside inverted regions can be obtained by modeling the renewal process with gamma-distributed distances initiated at heterozygous inversion breakpoints and scaled to cM of the standard genetic map of *D. melanogaster*. Here, I develop the theoretical framework for the interference hypothesis of recombination suppression in chromosomal inversion heterozygotes. First, I demonstrate how to generate quantitative predictions for suppressed recombination rates in any interval outside heterozygous inversion by integrating the decay-with-distance function defined by crossover interference theory. Then, I test this hypothesis with experimental data on crossing-over outside four different paracentric inversions of the right arm of chromosome 3 in *D. melanogaster*. Finally, I outline how the interference hypothesis of recombination suppression can be applied in cases beyond *Drosophila* inversions and interpreted in the context of biophysical models of crossover interference.

MATERIALS AND METHODS

Modeling framework

The interference hypothesis of recombination suppression proposes heterozygous inversion breakpoints possess chiasma-like properties altering the local synaptonemal complex structure such that recombination suppression is predicted to decay outside of heterozygous inversions in the same manner as the strength of crossover interference decays with genetic distance (z) measured in map units (i.e., cM of the standard genetic map). Decay-with-distance is modeled with a coincidence function $C(z)$ describing coefficients of coincidence in the limit where interval sizes shrink to zero, and the genetic distance between the intervals is z map units. (i.e., $C(z)$ is the instantaneous probability of crossing-over at distance z). If $\mu(z)$ is the conditional probability of crossing-over in an interval given a crossover event at distance z map units, and μ is the unconditional probability of crossing-over in that interval, then coefficients of coincidence are just points along the coincidence function $C(z) = \mu(z)/\mu$ (McPeek and Speed 1995). In the context of inversion heterozygosity, $C(z)$ is the instantaneous probability of crossing-over describing the decay of recombination suppression in genetic distance z map units. Critically, while $\mu(z)$ is the probability of crossing-over at distance of z map units from heterozygous inversion breakpoints, μ is the probability of crossing-over for that same interval in the absence of inversion heterozygosity (i.e., μ is scaled to cM of the standard genetic map). In this framework, the likelihood of the interference hypothesis of recombination suppression (hereafter denoted H_1*: interference hypothesis*) can be evaluated against both the null hypothesis (H_0*: no interference*) or constrained models of interference (H_2*: interference with centromere effect*) by simply altering the form of $\mu(z)$ in the coincidence function $C(z) = \mu(z)/\mu$.

Theoretical predictions

Quantitative predictions for the alternative hypotheses were generated by: 1) assuming heterozygous inversion breakpoints act as chiasmata, 2) modeling recombination suppression extending from breakpoints with a coincidence function $C(z) = \mu(z)/\mu$, 3) parameterizing a functional model of $\mu(z)$ with *D. melanogaster* specific values, and 4) integrating the coincidence function to calculate the expected recombination fraction for intervals outside of heterozygous inversions. Because recombination fraction is the number of recombinant progeny observed divided by the total number of progeny scored in a recombination experiment, integration of coincidence functions (i.e., the function describing the change in instantaneous probability of crossing-over) directly predicts the recombination fraction in a testcross. This procedure is illustrated in Fig. 2 for a medially placed paracentric inversion of the right arm of *D. melanogaster* chromosome 3 in order to establish both the functional form of coincidence and the color-coding scheme used for the three alternative hypotheses throughout this report (see Supplementary Information for detailed derivation of models and SI Fig. S1 for illustration of the functions converted from the intrinsic centimorgan scale to Megabases).

First, in Fig. 2A, the null hypothesis (H_0*: no interference*, shown in orange) is based on no interference due to inversion breakpoints. The corresponding coincidence function is modeled by a Poisson point process and is always equal to one ($\mu(z) = \mu$) outside of inverted regions (McPeek and Speed 1995). This null hypothesis gives an expected recombination rate (shaded area-under-the-curve) when heterozygous inversion breakpoints do not cause recombination suppression outside the inverted region but still fully suppress recombination inside the inverted region. Furthermore, because this coincidence function is the same underlying model in Haldane's mapping function, the expected recombination fraction is exactly equal to the *D. melanogaster* standard genetic map length for that interval (Haldane 1919).

Second, in Fig. 2B, the interference hypothesis (H_1: *interference hypothesis*, shown in purple) models recombination suppression extending from heterozygous inversion breakpoints as crossover interference. Here the coincidence function is based on a renewal process where distances in map units between heterozygous inversion breakpoints and crossover events follow a gamma distribution with both shape and rate parameters fitted to the strength of *D. melanogaster* crossover interference (Morgan et al. 1935; Weinstein 1936; Foss et al. 1993; McPeek and Speed 1995; Zhao et al. 1995).

Third, in Fig. 2C, the interference hypothesis incorporating a centromere effect (H_2*: interference hypothesis centromere effect*, shown in green), introduces the canonical assumption that crossover interference, and therefore recombination suppression, does not extend across *D. melanogaster* centromeres (Muller 1916; Graubard 1934; Stevens 1936). Stated simply, H_2 models recombination suppression with the renewal process (like H_1) for the inverted right arm of chromosome 3, and the absence of suppression with the Poisson process (like H_0) for the uninverted left arm of chromosome 3. To test these three alternative hypotheses (H_0*: no interference*, H_1*: interference hypothesis*, H_2*: interference with centromere effect*), their theoretical predictions were tested against experimental data for recombination suppression from four different cosmopolitan paracentric inversions of the right arm of chromosome 3 in *D. melanogaster*.

Stock construction

Five inbred lines each carrying a different cosmopolitan paracentric inversion *In(3R)K*, *In(3R)P*, *In(3R)C*, *In(3R)Mo*, or the *Standard* arrangement (as an inversion-free negative control) were drawn from the *Drosophila melanogaster* Genetic Reference Panel (DGRP) (Fig. 3, see SI Fig. S2 for Mb scale) (Mackay et al. 2012). Inversions and the inversion-fee negative control were identified by polytene chromosome squashes of third instar larva salivary glands and confirmed with PCR amplification of inversion breakpoints. Focal third chromosomes were isolated by balancer chromosome-assisted extraction and placed on a common, standard arrangement genetic background for the *X*, *Y*, mitochondrial, and second chromosomes (from DGRP line 399).

Three fully penetrant dominant phenotypic markers (Gl^1, Sb^1, and Dr^1) were selected due to their position relative to inversion breakpoints (Fig. 3, SI Fig. S2, and SI Table S1). These markers were introgressed onto both the inverted arrangements and the standard arrangement (negative control) followed by repeated backcrossing for a minimum of ten generations. Two exceptions were made, Dr^1 on *In(3R)Mo* and Sb^1 on *In(3R)P*, because >10,000 meioses failed to produce desired marker-inversion recombinants. Excepting combinations involving Dr^1 on *In(3R)Mo* and Sb^1 on *In(3R)P*, a derived series of stocks was generated with all possible pairwise and three-way marker/inversion combinations.

Independently, all three dominant markers (Gl^1, Sb^1, and Dr^1) were also introgressed into a sixth inbred line for use as a common tester strain (*Canton-S* which also has the standard arrangement). Similarly, a derived series of stocks with all pairwise combinations of markers on the *Canton-S* genetic background were generated so the common tester strain could be used in factorial design described below. Finally, the isogenic stock w^{1118}*; 6326; 6326* was used for outcrossing the F_1 experimental females (see SI Table S2 for full list of stocks).

Crossing design

To generate F_1 experimental genotypes, three virgin females of standard arrangement tester strain *Canton-S* were crossed to three males homozygous for a given gene arrangement: *Standard* (inversion-free negative control), *In(3R)K*, *In(3R)P*, *In(3R)C*, or *In(3R)Mo* and hereafter collectively referred to as *In(3R)x*. Virgin female F_1 experimental genotypes were selected and outcrossed to male w^{1118}*; 6326; 6326*. The progeny of this cross (F_2) were scored for recombination via dominant markers and non-disjunction via white-eyed patroclinous exceptions. Non-disjunction

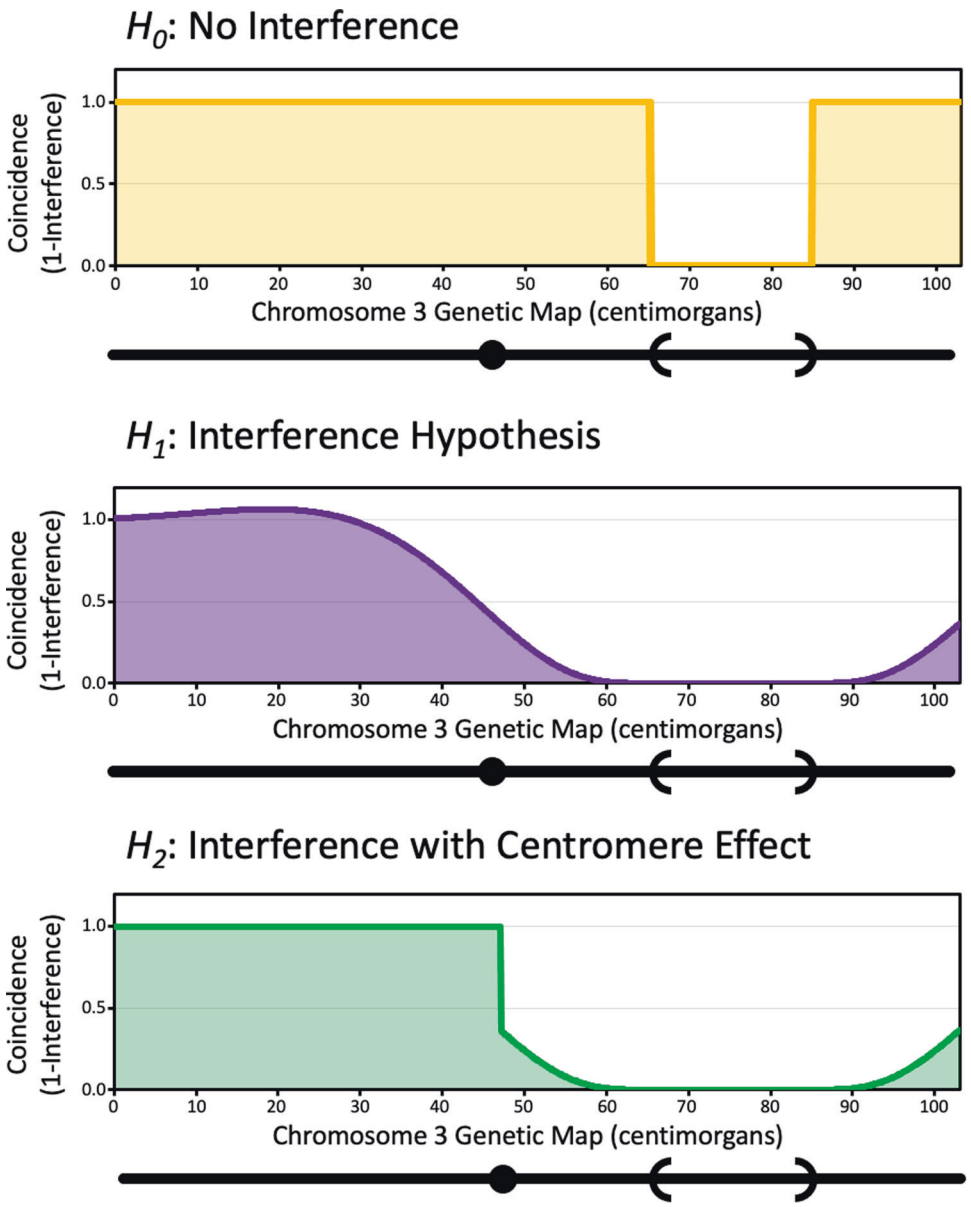

Fig. 2 Total chromosome-wide recombination phenotype. Three alternative coincidence functions are illustrated corresponding to the null hypothesis H_0: *no interference* (orange), H_1: *interference hypothesis* (purple), and H_2: *interference hypothesis with centromere effect* (green). The color-coded area-under-the-curve is equal to the predicted recombination fraction and was obtained by integrating the coincidence function. Alternative hypotheses are illustrated for a medially placed paracentric inversion of the right arm of chromosome 3 in *D. melanogaster*. The location of inversion breakpoints (parentheses) and centromere (circles) are shown on the chromosome diagram below each panel.

rates among gene arrangements do not differ with statistical significance ($F_{4,97} = 0.537$, $p = 0.709$) and were not considered further (SI Table S3).

A balanced design was employed to estimate recombination fractions while simultaneously controlling for viability effects of dominant phenotypic markers, genetic backgrounds, and the inversions themselves (Bodmer and Parsons 1959; Bailey 1961). This balanced design included both "marker-switching" and "cis-trans" recombination experiments with all possible marker-inversion combinations on a common genetic background. Four different crosses were performed to generate F_1 females with all markers and inversions in a full factorial design. In the *P* generation, virgin *Canton-S* females with marker genotypes Sb^+ Dr^+, Sb^1 Dr^+, Sb^+ Dr^1, or Sb^1 Dr^1 were mated with males homokaryotypic for one of the five gene arrangements [*Standard*, *In(3R)K*, *In(3R)P*, *In(3R)C*, or *In(3R)Mo*] carrying either Sb^1 Dr^1, Sb^+ Dr^1, Sb^1 Dr^+, or Sb^+ Dr^+, respectively. Thus, selected F_1 experimental females were always heterozygous for Dr^1, Sb^1, and *In(3R)x* in all possible linkage arrays on a common genetic background. For each gene arrangement, a second experiment was conducted independently following the same methods, but using Gl^1, Sb^1, and *In(3R)x* in all possible combinations.

Experimental conditions

Experimental conditions followed the standard methods for mapping established by Bridges and Brehme (1944). Five virgins of the desired F_1 genotype were collected over a three-day period, aged an additional three days, then outcrossed to five males from isogenic stock *6326*, which had the standard arrangement on all chromosome arms and the *X*-linked mutation w^{1118}. Crosses were conducted using light CO_2 anesthesia. After allowing 24 h for recovery, the mated group of ten individuals were tap transferred into half-pint bottles with 30–40 ml of standard cornmeal-agar *Drosophila* food. Three replicate bottles were set for each cross. After five days of egg laying the F_1 adults were removed from bottles. A 2.5-inch × 2.5-inch blotting paper square was added to provide ample pupation sites with 0.05% v/v propionic acid added as needed to hydrate food. Emerging progeny (F_2) were then scored daily for recombination (via dominant markers) and non-disjunction (via white-eyed patroclinous exceptions) for 15 days after the last eggs were laid. All vials and bottles were held at 25 °C, greater than 50% relative humidity, under 24-h light in a Percival Scientific incubator. Under these conditions, each bottle yields between 100 and

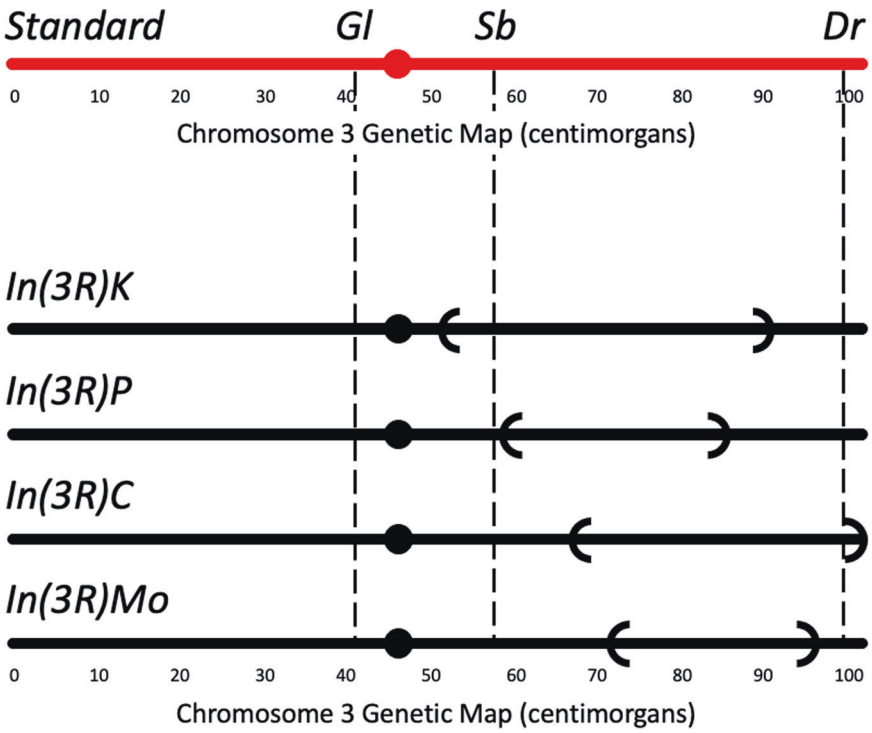

Fig. 3 Diagram of marker and inversions. The relative position of phenotypic markers (*Gl, Sb*, and *Dr*) to the centromere (closed circle) for the standard arrangement chromosome 3 in *D. melanogaster* as an inversion-free negative control is shown in red. The four cosmopolitan paracentric inversions of chromosome 3 right arm (shown in black) have their inversion breakpoint locations indicated by parentheses. Diagram is to scale based on the standard genetic map of *D. melanogaster*. For genomic, cytogenetic, and genetic map locations of markers and inversion breakpoints see SI Table S1.

1000 F_2 offspring for scoring. With a per locus gene conversion rate of 2.2×10^{-5}, ~2 in 44,230 total F_2 offspring should produce false positives due to gene conversion at a visible marker (Hilliker et al. 1994).

Statistical analysis

The crossing scheme outlined above yields a $2 \times 2 \times 2$ full factorial design with respect to markers and inversions advocated by Bodmer and Parsons (1959). With knowledge of the initial linkage phase in *P* genotypes, the frequency of each progeny phenotypic class can be further decomposed to include the effect of recombination. The experimental data can be described by a linear model with terms for the effect of recombinant class, and the viability of each marker, gene arrangement, and all possible two-way and three-way interactions of viability effects (SI Eqs. S6 and S7) (Bodmer and Parsons 1959; Bailey 1961). After angular transformation $\theta = \sin^{-1}\sqrt{p}$ to meet error term normality assumptions, the data was analyzed by ANOVA using type II sum of squares (Sokal and Rohlf 1995). Recombination data for intervals *Gl-Sb* and *Sb-Dr* were collected independently and, therefore, analyzed separately.

Effects of markers and gene arrangements were reported as relative viabilities compared to wildtype and the standard gene arrangement of *Canton-S* (the common tester strain), respectively (SI Table S4). Both raw counts and viability-corrected recombination fractions are reported, the latter represents an unbiased estimate of the recombination rate based on a linear model corresponding to the factorial experimental design. Basing the estimated recombination rate on back-transformed fitted values for each phenotypic class accounts for the confounding viability effects of markers, inversions, and their potential interaction; therefore, in the rest of this study, this unbiased estimate is referred to as the viability-corrected recombination rate (SI Tables S5–S14). Please see Supplementary Information for detailed description of all linear models and analyses.

Analysis of model fit

To assess which of the alternative hypotheses of recombination suppression (H_0: *no interference*, H_1: *interference hypothesis*, H_2: *interference with centromere effect*) best fit the data, the viability-corrected observed recombination rates were compared to their theoretically predicted values under each of the alternative hypotheses. For reference, Fig. 4 provides graphical representation of the theoretical predictions for all three alternative hypotheses (from Fig. 2) applied to each inversion (from Fig. 3). In Fig. 4, the predicted recombination rate for intervals *Gl-Sb* and *Sb-Dr* is exactly equal to the color-coded area-under-the-curve bound by the position of visible markers (shown as dotted lines). In this framework, the curve is the coincidence function describing how the instantaneous probability of crossing-over decays to a wild-type baseline with genetic distance from heterozygous inversion breakpoints; as such, integration of this function for a specified interval is exactly equal to the theoretically predicted recombination rate for that interval (SI Eqs. S2, S3). For illustrative purposes only, SI Fig. S3 provides these functions rescaled from cM to Mb.

To formalize the model fit, predictions from the three hypotheses (H_0: *no interference*, H_1: *interference hypothesis*, H_2: *interference with centromere effect*) were compared to observations using the likelihood function for the binomial distribution. Because each model of recombination suppression is an extrinsic hypothesis with zero parameters estimated from the data, the alternative hypotheses could be directly compared with log-likelihoods. Log-likelihoods for all inversions, intervals, and models are reported so the specific intervals and inversions causing lack-of-fit under each hypothesis could be identified by examining the marginal tables of log-likelihoods. Only the viability-corrected recombination rates were used in log-likelihood calculations reported here, although raw recombination fraction yield comparable likelihoods. For detailed description of statistical models, parameterization, and predictions for alternative hypotheses of recombination suppression see Supplementary Information.

RESULTS

The full set of ten experiments scored the result of 44,230 meioses for crossing-over in two intervals on five gene arrangements [*Standard*, *In(3R)K*, *In(3R)P*, *In(3R)C*, and *In(3R)Mo*], consisting of 102 experimental F_1 bottles. Specific genotypes, karyotypes, marker arrays, and raw count data for each of the 102 experimental bottles are provided in Supplementary Information File 1. Under the described experimental conditions, the raw recombination fractions for inversion-free negative control

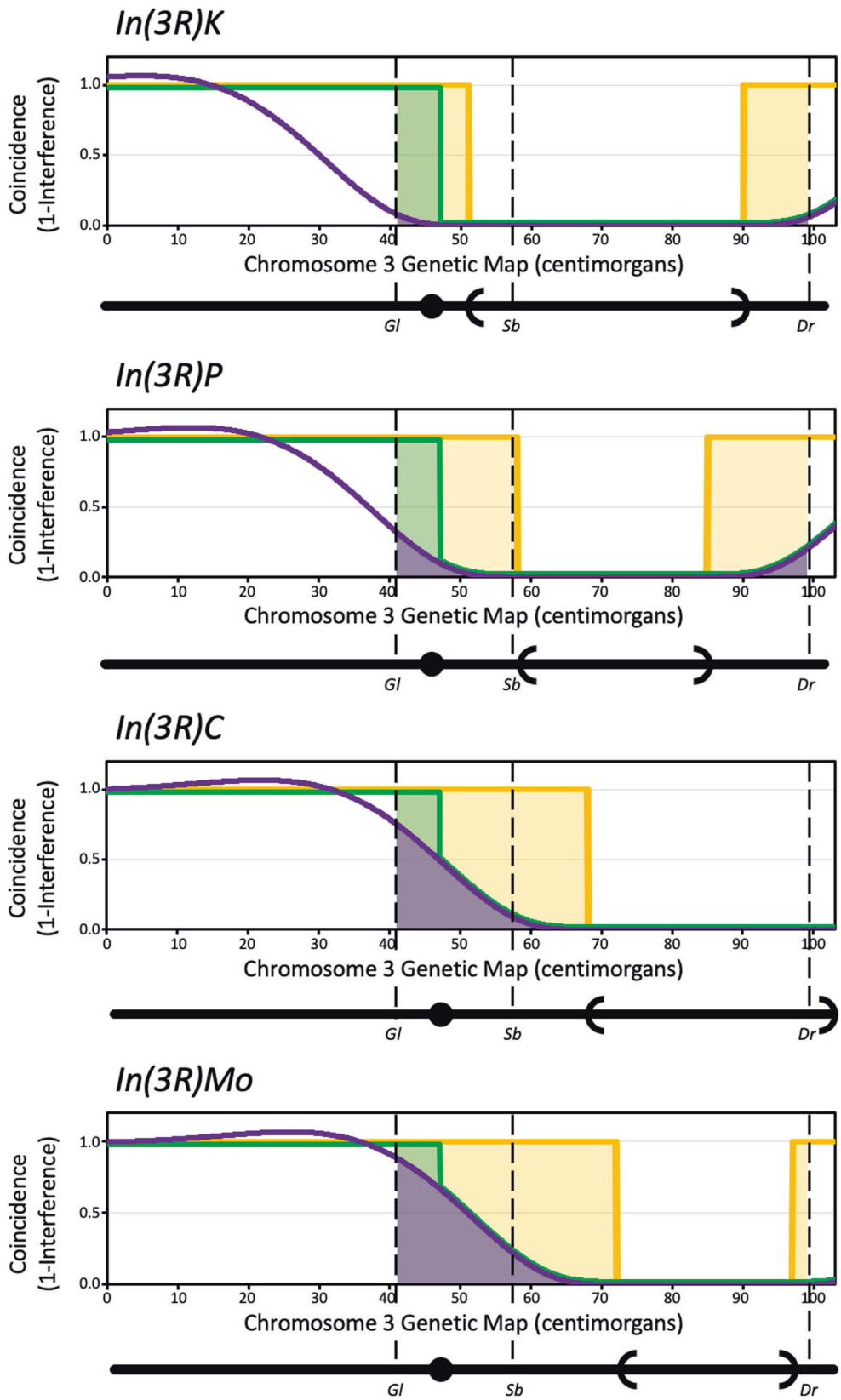

Fig. 4 Illustration of predicted recombination fractions. Expected recombination fractions for the null hypothesis H_0: *no interference* (orange), H_1: *interference hypothesis* (purple), and H_2: *interference hypothesis with centromere effect* (green) are illustrated as color-coded area-under-the-curve bound by black dotted lines representing location of visible markers. Corresponding values are reported as expected values in Table 1. The location of inversion breakpoints for *In(3R)K*, *In(3R)P*, *In(3R)C*, and *In(3R)Mo* (in order top to bottom) are shown by parentheses on chromosome diagram below each respective panel.

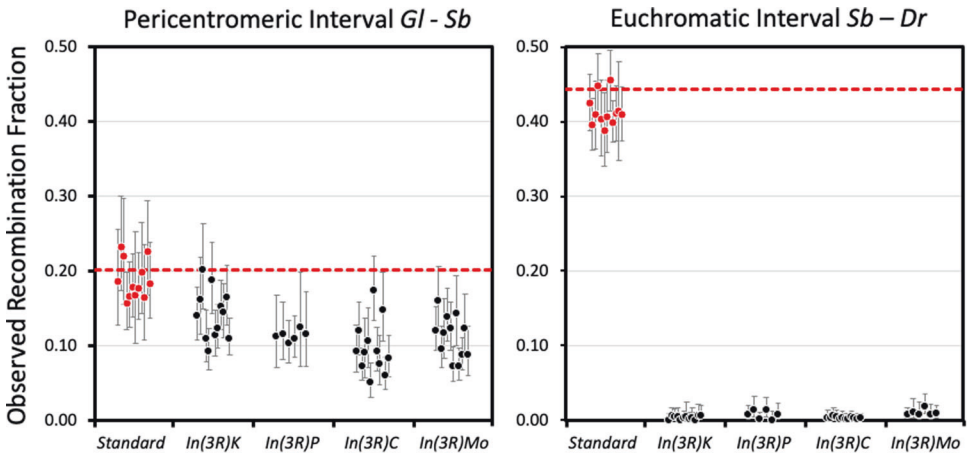

Fig. 5 Model-free comparison of raw recombination fractions. The observed recombination fractions, with exact 95% confidence intervals, for all 102 experimental bottles in this study. The 102 bottles included experiments on two intervals of *D. melanogaster* chromosome 3 (cf. Fig. 3), a pericentromeric region (left panel) and right arm euchromatic region (right panel). The raw recombination fractions for the inversion-free negative control (*Standard*, shown as red dots), and its viability-corrected estimate (red dotted line), was always greater than the suppressed recombination fractions observed in the presence of inversion heterozygosity for *In(3R)K*, *In(3R)P*, *In(3R)C*, and *In(3R)Mo* (listed in order of proximity to the centromere with raw data shown as black dots).

Table 1. Expected and observed recombination experiment results.

Inversion	Interval	H_0: Expected	H_1: Expected	H_2: Expected	Sample Size	Raw Observed	Viability-Corrected
In(3R)K	*Gl-Sb*	477 (0.10)	9 (0.0018)	287 (0.060)	4774	644 (0.14)	710 (0.15)
In(3R)K	*Sb-Dr*	446 (0.090)	9 (0.0018)	9 (0.0018)	4960	15 (0.0030)	12 (0.0024)
In(3R)P	*Gl-Sb*	301 (0.17)	26 (0.015)	111 (0.063)	1771	196 (0.11)	197 (0.11)
In(3R)P	*Sb-Dr*	334 (0.14)	17 (0.0071)	17 (0.0071)	2389	17 (0.0071)	13 (0.0053)
In(3R)C	*Gl-Sb*	735 (0.17)	290 (0.067)	386 (0.089)	4324	400 (0.093)	422 (0.098)
In(3R)C	*Sb-Dr*	836 (0.10)	15 (0.0018)	15 (0.0018)	8364	24 (0.0029)	19 (0.0022)
In(3R)Mo	*Gl-Sb*	929 (0.17)	516 (0.095)	587 (0.11)	5463	578 (0.11)	624 (0.11)
In(3R)Mo	*Sb-Dr*	478 (0.16)	21 (0.0071)	21 (0.0071)	2985	31 (0.010)	28 (0.0095)

Counts of recombinants are given with corresponding recombination rates listed parenthetically. Expected results under null hypothesis of H_0: *no interference*, H_1: *interference hypothesis*, and H_2: *interference hypothesis with centromere effect*, are compared to both raw observations and the viability-corrected recombination rates.

(standard arrangement homozygote) were consistent with the standard FlyBase genetic map. This result validated the experimental conditions and justified the use of standard genetic map units to generate expected recombination fraction between inversion breakpoints and phenotypic markers under alternative hypotheses. Importantly, a model-free comparison of the 78 raw recombination fractions in the presence of inversion heterozygosity to the 24 inversion-free negative controls cannot test the interference hypothesis, it simply establishes that some form of spatial redistribution of crossing-over occurs due to the introduction of inversions.

Figure 5 illustrates the raw observed recombination fractions (with exact 95% confidence intervals) for all 102 experimental bottles including the inversion-free negative control (*Standard*, shown as red dots) and four different inversions of the right arm of chromosome 3 in *D. melanogaster* [*In(3R)K*, *In(3R)P*, *In(3R)C*, and *In(3R)Mo*, shown as black dots]. The model-free visualization of data in Fig. 5 serves to highlight three important features of the raw data. First, recombination rates for both pericentromeric and euchromatic regions were always suppressed in inversion heterozygotes relative to the inversion-free negative control (viability-corrected average of the standard arrangement homozygotes is extended as dotted red line in Fig. 5). Second, recombination rates were much lower in the euchromatic interval because this interval encompasses some, or all, of the inverted regions of the chromosome (right panel Fig. 5). Third, there is a large degree of variability both intrinsic to recombination rate data (illustrated by 95% confidence intervals for a given bottle) and among biological replicates (comparing different bottles for the same gene arrangement).

To extract an unbiased estimate of experimental recombination rates requires modeling the intrinsic variability of raw recombination fractions as well as accounting for the confounding viability effects of markers, inversions, and their potential interactions. Among the ten independent experiments in this study, viability effects of both markers and inversions were common (10 of 27), as were statistically significant interactions (4 instances), and none of these effects were of uniform magnitude across experiments (SI Table S4). Therefore, viability-corrected recombination rates were estimated from the full linear models describing raw recombination fractions while accounting for viability effects of marker, inversions, and their interactions in the corresponding factorial design (Bodmer and Parsons 1959; Bailey 1961). A summary of both raw counts and viability-corrected recombination rates is provided in Table 1 (for full ANOVA tables see SI Tables S5–S14). Although these viability corrections were small, the intrinsic variability in recombination experiments (cf. Fig. 5), and the precision of the predicted recombination rates (cf. Table 1), highlight the importance of both balanced experimental design and modeling the data in recombination experiments designed to test alternative hypotheses in a statistical framework (Bailey 1961).

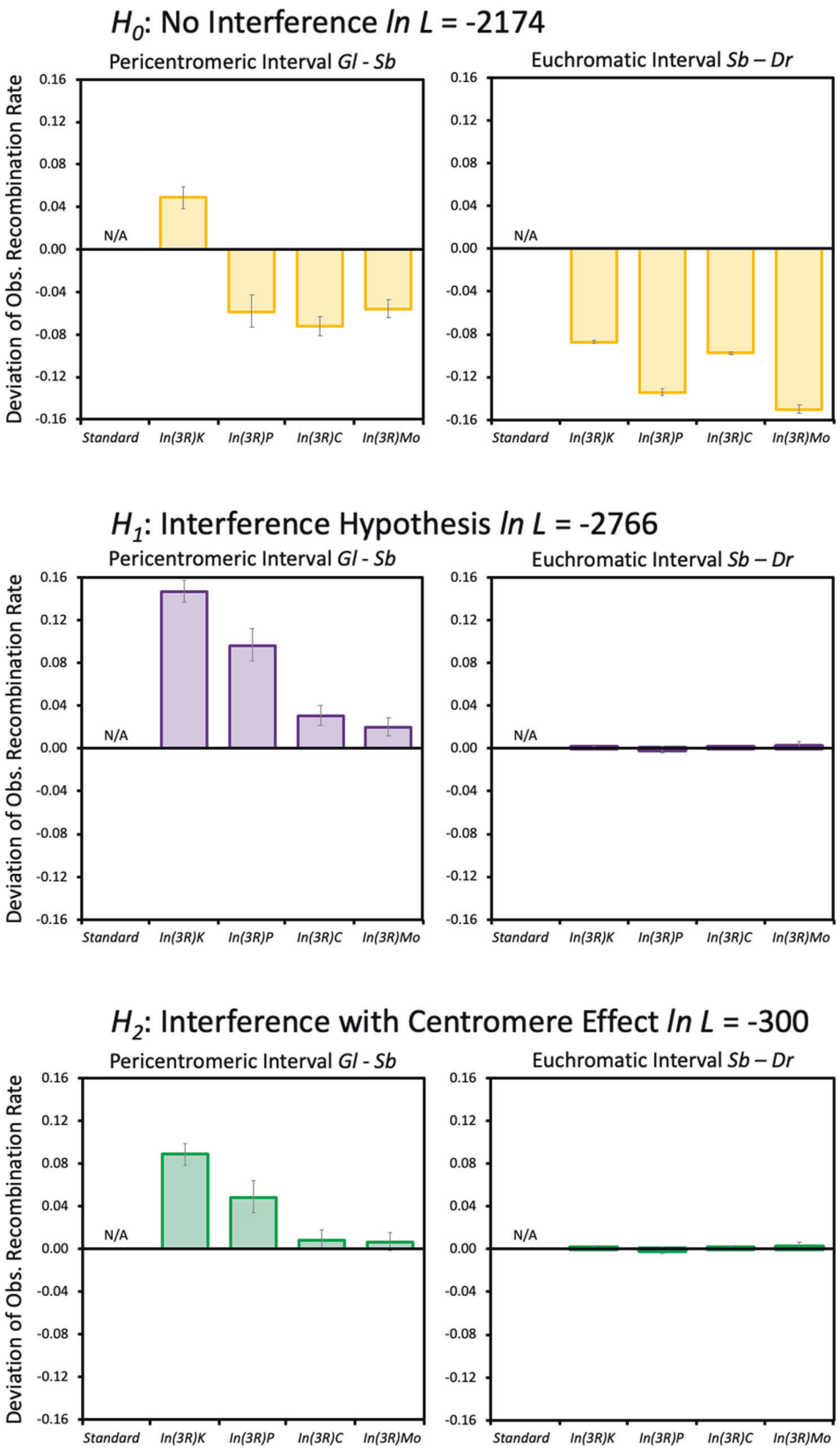

To test the alternative hypotheses of recombination suppression (H_0: *no interference*, H_1: *interference hypothesis*, H_2: *interference with centromere effect*), the observed viability-corrected recombination rates were compared to their model-derived expected values. Figure 6 illustrates this comparison by plotting deviations of the observed values from their expected values on an arithmetic scale for each inversion, in each interval (left vs. right), and each of the three hypotheses (H_0: orange on top,

Fig. 6 Deviation of observed recombination rates from model-based predictions. The three color-coded alternative hypotheses (H_0: orange, H_1: purple, and H_2: green) were evaluated by plotting the deviation of observed viability-corrected recombination rates from their model-based expected values, with exact 95% confidence intervals based on all biological replicates (cf. Table 1). Deviations for *In(3R)K*, *In(3R)P*, *In(3R)C*, and *In(3R)Mo* are shown in order of proximity to the centromere, with "not applicable" (N/A) representing the absence of an expected value in *Standard* arrangement homozygotes. Graphically, larger deviations from zero indicate poorer model fit; statistically, model fit was reported as log-likelihood of each hypothesis. H_0: *no interference* (orange) did not describe suppressed recombination outside of inversions in any interval (ln $L = -2174$, top left and right panels). H_1: *interference hypothesis* (purple) made highly accurate predictions in the euchromatic interval but failed in pericentromeric regions (ln $L = -2766$, middle right vs. left panels). H_2: *interference with centromere effect* (green) provided the overall best explanation, preserving the highly accurate euchromatic predictions of H_1 and uniformly improving fit in pericentromeric intervals (ln $L = -300$, bottom left and right panels). Under both H_1 and H_2, the two most centromere proximal inversions, *In(3R)K* and *In(3R)P*, were responsible for vast majority of excess recombination.

H_1: purple in the middle, H_2: green on bottom). SI Fig. S4 plots variation in both observations and expectations but requires a logarithmic scale to visualize the simultaneous comparison of inversions, intervals, and hypotheses.

To evaluate the overall fit of the three hypotheses, the following question is posed: "What is the likelihood of hypothesis H_0 versus H_1 versus H_2 given the viability-corrected recombination fractions observed?" The overall likelihoods of H_0 (ln $L = -2174$) and H_1 (ln $L = -2766$) were similar and indicated relatively poor fits because a more negative value means a lower likelihood that the observed values were generated from the specified model. However, a closer inspection of marginal likelihoods in Table 2 and graphical deviations in Fig. 6 reveals that the null hypothesis H_0: *no interference* was a poor fit for all inversions in both intervals. In contrast, H_1: *interference hypothesis* was an extraordinarily good fit for all inversions in the euchromatic interval *Sb-Dr*, where it predicted the number of recombinants with an error of only 3–8 flies in experiments with 2000–9000 individuals. Consequently, 81% of deviations from H_1 expected values were confined to the pericentromeric interval *Gl-Sb* and caused by just the two most proximally placed inversions [*In(3R)K* and *In(3R)P*, Fig. 6 middle left panel].

Constraining recombination suppression to the inverted chromosome arm (i.e., assuming suppression does not extend across the centromere as stated in H_2: *interference hypothesis with centromere effect*) dramatically improved the interference hypothesis overall fit in the pericentromeric intervals for all four inversions (Fig. 6 bottom left panel). The constrained model of H_2 accounts for 44% of excess recombination detected in pericentromeric interval *Gl-Sb* in the unconstrained model of H_1: *interference hypothesis*. Assuming crossover interference does not extend across the centromere is the canonical assumption in *D. melanogaster* (Stevens 1936; Pazhayam et al. 2021), and incorporating this assumption into the analysis *via* H_2: *interference hypothesis with centromere effect* produced the greatest likelihood (ln $L = -300$) given the observed viability-corrected recombination rates.

Similar to the deviations from H_1 expectations, 87% of total deviation from H_2 was higher than expected recombination in the pericentromeric interval caused by the two most proximally placed inversions [*In(3R)K* and *In(3R)P*, Fig. 6 bottom left panel]. This relatively small, residual excess recombination in pericentromeric intervals is consistent with the action of negative suppression and, by analogy, negative crossover interference extending across *D. melanogaster* centromeres. Negative crossover interference is the uncommon observation of an increased, rather than decreased, probability of crossing-over in an interval given a crossover event nearby. Negative crossover interference is rarely incorporated into mapping functions; however, its presence at *D. melanogaster* centromeres and associate pericentric heterochromatin has been reproducibly observed and extensively documented (Morgan et al. 1925; Green 1975; Sinclair 1975; Denell and Keppy 1979).

Table 2. Marginal tables for log-likelihood values.

A) H_0: No Interference

Inversion	*Gl-Sb*	*Sb-Dr*	Sums
In(3R)K	−60	−413	−473
In(3R)P	−28	−305	−333
In(3R)C	−96	−791	−887
In(3R)Mo	−71	−411	−482
Sums	−254	−1920	−2174

B) H_1: Interference Hypothesis

Inversion	*Gl-Sb*	*Sb-Dr*	Sums
In(3R)K	−2478	−3	−2481
In(3R)P	−228	−3	−231
In(3R)C	−33	−3	−35
In(3R)Mo	−16	−4	−19
Sums	−2755	−12	−2766

C) H_2: Interference with Centromere Effect

Inversion	*Gl-Sb*	*Sb-Dr*	Sums
In(3R)K	−245	−3	−247
In(3R)P	−33	−3	−35
In(3R)C	−6	−3	−8
In(3R)Mo	−5	−4	−9
Sums	−288	−12	−300

Likelihood of A) null hypothesis H_0: *no interference*, B) H_1: *interference hypothesis*, and C) H_2: *interference hypothesis with centromere effect*, given the viability-corrected recombination rates.

DISCUSSION

Recombination suppression in chromosomal inversion heterozygotes is a complex phenotype that varies in magnitude and extent both inside and outside of inverted regions. The interference hypothesis of recombination suppression states that heterozygous inversion breakpoints possess chiasma-like properties altering local synaptonemal complex structure such that recombination suppression extends from these breakpoints in a process analogous to crossover interference. This hypothesis, first proposed by Gong et al. (2005), is qualitatively consistent with chromosome-wide redistribution of crossover events and has the potential to unify various regional suppression effects under a single mechanism.

In the present study, quantitative predictions for the interference hypothesis of recombination suppression were derived from statistical models of crossover interference. To test these predictions, a balanced experimental design was employed to estimate viability-corrected recombination fractions for each of four inversions of the right arm of chromosome 3 in *D. melanogaster* (Fig. 4).

These experiments revealed: 1) highly accurate a priori prediction of recombination rates in euchromatic intervals for all inversions, 2) slightly higher than expected recombination in pericentromeric intervals for all inversions, and 3) inversions closer to the centromere tended to have greater excess recombination in pericentromeric intervals. Finally, likelihood analysis supports a model of recombination suppression where the interference-like effects from heterozygous breakpoints are constrained to the inverted chromosome arm and do not extend across the centromere (Fig. 6 and Table 2). The precise prediction of recombination suppression in euchromatic intervals is the most notable result presented here; however, the excess recombination observed in pericentromeric intervals was the most unexpected finding. Detection of this excess was only possible with precise quantitative predictions from the interference hypothesis (H_1: Fig. 6 middle left panel). Introducing the formal assumption that positive crossover interference does not extend across the centromere explains 44% of excess recombination in pericentromeric intervals (H_2: Fig. 6 bottom left panel). The remaining 56% of excess recombination could either be due to the intrachromosomal effect, crossover homeostasis, altered chromatin dynamics, or negative crossover interference in pericentromeric regions.

Exploratory analysis of recombination suppression

The excess recombination in pericentromeric intervals observed here is unlikely to be the same intrachromosomal effect observed by Ramel (1968). Ramel's (1968) intrachromosomal effect only increased recombination in medial and distal intervals of the uninverted arm, while leaving the intervening pericentromeric intervals unchanged or with lowered recombination rates. The results presented here also suggest crossover homeostasis is an unlikely explanation of excess recombination in pericentromeric intervals. The recombination in pericentromeric interval *Gl-Sb* was not anticorrelated with either recombination in euchromatic interval *Sb-Dr* or with the size of the inverted region, as would be expected under homeostatic models SI Fig. S5 (Martini et al. 2006; Sidhu et al. 2015; Wang et al. 2015).

In principle, reduced rates of crossing-over per μm of the chromosome axis in the pericentromeric heterochromatin could make crossover interference decay more rapid when scaling to the standard genetic map (as performed here). However, altered chromatin-dependent dynamics in the context of the present study would affect all four inversions tested, and substantial excess recombination was only observed for the two inversions with breakpoints closest to the pericentromeric heterochromatin (left panels Fig. 6). Indeed, excess recombination was strongly anti-correlated ($r = -0.99$) with genetic distance from the proximal inversion breakpoint to the centromere (SI Fig. S5 right panel). Thus, while the improved fit of *H_2: interference hypothesis with centromere effect* over *H_1: interference hypothesis [without centromere effect]* may be related to chromatin packing in the pericentromeric interval, the excess recombination above and beyond the predictions of H_2 appears to be due to heterozygous inversion proximity to pericentromeric heterochromatin and is consistent with negative crossover interference extending across the centromere.

In *D. melanogaster*, crossing-over on one euchromatic arm of a metacentric chromosome does not generally alter the probability of observing crossover events for the other euchromatic arm (Muller 1916; Graubard 1934; Stevens 1936; Miller et al. 2016a); however, when relatively rare pericentromeric crossover events occur on one arm there is, paradoxically, an increased probability of crossing-over in the opposite arm's pericentromeric region (Morgan et al. 1925; Green 1975; Sinclair 1975; Denell and Keppy 1979). This effect can be quite strong, with empirical coefficients of coincidence exceeding unity by several orders of magnitude, causing correspondingly negative values for strength of inference. Negative crossover interference occurring at centromeres predicts that heterozygous inversion breakpoints in the pericentromeric region of one arm would promote, rather than suppress, recombination in the pericentromeric region of the opposite arm. Future experiments capable of partitioning the pericentromeric *Gl-Sb* recombination rates into left arm heterochromatin and right arm heterochromatin may quantify the strength of such negative crossover inference. Nevertheless, the experimental results presented here demonstrate: 1) the excess recombination in pericentromeric intervals are greater for inversions closer to the centromere (bottom left panel Fig. 6), and 2) the excess magnitude is predicted by distance from proximal inversion breakpoint to centromere (bottom left panel Fig. 6, SI Fig. S5 right panel). Both of these findings are consistent with a negative recombination suppression due to heterozygous inversion breakpoints that can extend across the centromere, and, conversely, the likelihood analysis indicates positive recombination suppression due to heterozygous inversion breakpoints is constrained to the inverted chromosome arm. Notably, this scenario is analogous to the properties of negative and positive crossover interference at centromeres of *D. melanogaster*.

Further application of the interference hypothesis

The analysis presented here focused on recombination suppression outside heterozygous paracentric inversions in *D. melanogaster*, but the interference hypothesis can be applied to a wide range of chromosomal regions, different rearrangements, and various experimental organisms. As noted in the Introduction, only one-fourth of recombination suppression observed inside inverted regions is due to eliminatiion of acentric/dicentric chromatids (Sturtevant and Beadle 1936; Novitski and Braver 1954), and the unexplained fraction can be predicted by modeling the internal decay-with-distance from heterozygous inversion breakpoints. Modeling of coincidence functions inside inversions is complicated by the interaction of interference extending inward from both proximal and distal breakpoints, but once derived, these functions generate simple predictions for recombination fractions that can be experimentally tested using compound chromosomes.

The interference hypothesis can also be applied to pericentric inversions and translocations, the heterozygous breakpoints of which are expected to introduce discontinuities in the synaptonemal complex and produce similar recombination suppression in *D. melanogaster* (Glass 1933, Alexander 1952; Roberts 1967, 1972). Analysis of paracentric inversions presented here revealed assumptions about crossover interference at centromeres proved to be the largest determinant of model fit. Existing models of whole chromosome crossover patterning have not incorporated the assumption that positive crossover interference (between euchromatic arms) does not cross the centromere, while negative crossover interference (between pericentromeric regions) does cross the centromere (Muller 1916; Graubard 1934; Stevens 1936; Denell and Keppy 1979; Berchowitz and Copenhaver 2010; Pazhayam et al. 2021). Therefore, particular attention should be given to breakpoint proximity to pericentromeric heterochromatin when generating predictions for chromosomal rearrangements that involve multiple chromosomal arms (i.e., pericentric inversions and reciprocal translocations).

The interference hypothesis of recombination suppression is testable in any sexually reproducing system requiring only: 1) meiosis, 2) chromosomal rearrangements, and 3) the ability to measure crossing-over (either cytologically or with genetic markers). This includes traditional genetic model organisms [e.g., *S. cerevisiae* (Dresser et al. 1994), *A. thaliana* (Termolino et al. 2019), *C. elegans* (Zetka and Rose 1992) *Mus spp*. (Hammer et al. 1989)] as well as an ever-expanding list of non-model organisms [e.g., anther-smut fungi (Duhamel et al. 2022), barley (Farré et al. 2012), salmon (Stenløkk et al. 2022), sparrows (Thomas et al. 2008)]. The first step in adapting the hypothesis to

a new system is estimating strength of crossover interference in absence of structural heterozygosity and testing for presence of the non-interferring (type II) crossover pathway (Copenhaver et al. 2002; Housworth and Stahl 2003; Basu-Roy et al. 2013). Hypothesis testing can follow the mathematical framework established in the present study, but differences among species in crossover interference strength and proportion of type II crossovers will determine the precise decay-with-distance of the predicted recombination suppression.

Further interpretation of the interference hypothesis

Interference hypotheses and their model-derived predictions are a major advancement in studying the effects of inversion heterozygosity because they make explicit predictions for the magnitude and extent of recombination suppression outside inverted regions as well as the chromosome-wide modification of crossover distribution (Navarro et al. 1997; Gong et al. 2005; this study). However, the statistical analysis of the interference hypothesis presented here cannot provide direct evidence of a mechanistic link between crossover interference and recombination suppression. Indeed, the mechanism of crossover interference remains unknown, with several authors suggesting interference is only one facet of an integrated crossover patterning mechanism that is also responsible for crossover assurance, crossover homeostasis, and centromere effects (Berchowitz and Copenhaver 2010; Zhang et al. 2014a; Wang et al. 2015; Pazhayam et al. 2021). Biophysical hypotheses [e.g., the reaction-diffusion model (Fujitani et al. 2002; Stauffer et al. 2019), beam-film model (Kleckner et al. 2004; Zhang et al. 2014a), and liquid-crystal model (Rog et al. 2017; Zhang et al. 2018)] hold much promise for integrating statistical patterns of crossing-over with the underlying cellular mechanisms (Otto and Payseur 2019; Pazhayam et al. 2021; von Diezmann and Rog 2021).

The full chromosome-wide patterning phenotype, both crossover distibution and non-crossover gene conversion events, can now be readily quantified with low-coverage whole-genome sequencing (Miller et al. 2016c; Crown et al. 2018). Such studies should help clarify many of the poorly understood statistical patterns in classical studies, including the ratio of crossover to non-crossover gene conversion events that is at the core of counting, chi-square, and gamma models of crossover interference (Foss et al. 1993; Zhao et al. 1995; McPeek and Speed 1995), and is potentially causing the interchromosomal effect of inversion heterozygosity (Crown et al. 2018). Establishing a mathematical framework for recombination suppression in structural heterozygotes at a chromosome-wide level (both inside and outside of inverted regions, near breakpoints, across centromeres, and in any sexually-reproducing experimental system) opens up the possibility of incorporating various cytological observations on pairing heterogeneity and synaptonemal complex discontinuity in a systematic way to derive directly testable predictions from this large cytogenetic knowledge base (Parker 1987; Page and Hawley 2001; Gong et al. 2005; Zhang et al. 2014; Termolino et al. 2019).

In particular, the statistical results of the present study can be interpreted in context of a dynamical model proposing initially uniform pro-crossover factors diffusing in synaptonemal complex undergo a "coarsening" process during pachytene to produce the regularly patterned crossover events (Zhang et al. 2018; Morgan et al. 2021; Durand et al. 2022). The interference hypothesis of recombination suppression, as stated here, treats heterozygous inversion breakpoints like obligate chiasmata such that pro-crossover factors coalesce at these sites at the expense of the flanking chromosomal regions where recombination is suppressed. However, an alternative coarsening model interpretation is that a synaptonemal complex discontinuities at heterozygous inversion breakpoints produce recombination suppression by limiting free diffusion of pro-crossover factors near inversion breakpoints. In principle, these alternatives generate different decay-with-distance functions for recombination suppression that could be differentiated with sufficiently large experimental designs or direct measurement of diffusion.

Future investigations should focus on the potential of different chromatin packing in pericentromeric heterochromatin that may alter the diffusion of pro-crossover factors or propagation dynamics of crossover interference signals and, by extension, recombination suppression. Interestingly, synaptonemal complex structural differences at *D. melanogaster* pericentric heterochromatin have previously been observed (Carpenter 1975), further highlighting the need for special treatment of this region with respect to the interference hypothesis. Synthesis of biophysical and statistical models of the crossover patterning mechanism can be mostly readily achieved by focusing on the special cases, such as inversion heterozygosity, where precise a priori statistical, cytological, and biophysical predictions can be generated for the same experimental system.

DATA ARCHIVING

The raw data underlying this article are available in the online Supplementary Information File 1. Full ANOVA tables for each recombination experiment conducted are included in Supplemental Information as SI Tables S5–S14. The raw data available in Supplementary Information File 1 is further archived in the Dryad data repository: https://doi.org/10.5061/dryad.cc2fqz69t.

REFERENCES

Alexander ML (1952) The effect of two pericentric inversions upon crossing over in *Drosophila melanogaster*. Univ Tex Publ 5204:219–226

Bailey NTJ (1961) Introduction to the mathematical theory of genetic linkage. The Clarendon Press, Oxford

Basu-Roy S, Gauthier F, Giraut L, Mézard C, Falque M, Martin OC (2013) Hot regions of noninterfering crossovers coexist with a nonuniformly interfering pathway in *Arabidopsis thaliana*. Genetics 195:769–779

Berchowitz LE, Copenhaver GP (2010) Genetic interference: don't stand so close to me. Curr Genom 11:91–102

Bodmer WF, Parsons PA (1959) The analogy between factorial experimentation and balanced multi-point linkage tests. Heredity 13:145–156

Brand CL, Larracuente AM, Presgraves DC (2015) Origin, evolution, and population genetics of the selfish Segregation Distorter gene duplication in European and African populations of *Drosophila melanogaster*. Evolution 69:1271–1283

Bridges CB, Brehme KF (1944) The mutants of *Drosophila melanogaster* Carnegie Institution of Washington, Washington D.C

Capilla-Pérez L, Durand S, Hurel A, Lian Q, Chambon A, Taochy C, et al. (2021) The synaptonemal complex imposes crossover interference and heterochiasmy in Arabidopsis. Proc Natl Acad Sci 118

Carpenter ATC (1975) Electron microscopy of meiosis in *Drosophila melanogaster* females. Chromosoma 51:157–182

Carson HL (1946) The selective elimination of inversion dicentric chromatids during meiosis in the eggs of *Sciara impatiens*. Genetics 31:95

Cobbs G (1978) Renewal process approach to the theory of genetic linkage: case of no chromatid interference. Genetics 89:563–581

Copenhaver GP, Housworth EA, Stahl FW (2002) Crossover interference in Arabidopsis. Genetics 160:1631–1639

Crown KN, Miller DE, Sekelsky J, Hawley RS (2018) Local inversion heterozygosity alters recombination throughout the genome. Curr Biol 28:2984–2990

Denell RE, Keppy DO (1979) The nature of genetic recombination near the third chromosome centromere of *Drosophila melanogaster*. Genetics 93:117–130

von Diezmann L, Rog O (2021) Let's get physical–mechanisms of crossover interference. J Cell Sci 134:jcs255745

Dobzhansky T (1931) The decrease of crossing-over observed in translocations, and its probable explanation. Am Nat 65:214–232

Dobzhansky T (1933) Studies on chromosome conjugation. Z Indukt Abstamm Vererb 64:269–309

Dobzhansky T, Sturtevant AH (1931) Translocations between the second and third chromosomes of Drosophila and their bearing on Oenothera problems. Pub Carnegie Instn Washing 421:39–59

Dresser ME, Ewing DJ, Harwell SN, Coody D, Conrad MN (1994) Nonhomologous synapsis and reduced crossing over in a heterozygous paracentric inversion in *Saccharomyces cerevisiae*. Genetics 138:633–647

Duhamel M, Carpentier F, Begerow D, Hood ME, Rodrıguez de la Vega RC, Giraud T (2022) Onset and stepwise extensions of recombination suppression are common in mating-type chromosomes of Microbotryum anther-smut fungi J Evol Biol 35:1619–1634

Durand S, Lian Q, Jing J, Ernst M, Grelon M, Zwicker D et al. (2022) Joint control of meiotic crossover patterning by the synaptonemal complex and HEI10 dosage. Nat Commun 13:1–13

Farré A, Cuadrado A, Lacasa-Benito I, Cistué L, Schubert I, Comadran J et al. (2012) Genetic characterization of a reciprocal translocation present in a widely grown barley variety. Mol Breed 30:1109–1119

Foss E, Lande R, Stahl FW, Steinberg CM (1993) Chiasma interference as a function of genetic distance. Genetics 133:681–691

France MG, Enderle J, Röhrig S, Puchta H, Franklin FCH, Higgins JD(2021) ZYP1 is required for obligate cross-over formation and cross-over interference in Arabidopsis. Proc Natl Acad Sci 118:e2021671118

Fujitani Y, Mori S, Kobayashi I (2002) A reaction-diffusion model for interference in meiotic crossing over. Genetics 161:365–372

Glass HB (1933) A study of dominant mosaic eye-colour mutants in *Drosophila melanogaster*. II. Tests involving crossing-over and non-disjunction. J Genet 28:69–112

Gong WJ, McKim KS, Hawley RS (2005) All paired up with no place to go: pairing, synapsis, and DSB formation in a balancer heterozygote. PLoS Genet 1:e67

Graubard MA (1934) Temperature effect on interference and crossing over. Genetics 19:83

Green MM (1975) Conversion as a possible mechanism of high coincidence values in the centromere region of Drosophila. Mol Gen Genet 139:57–66

Grell RF (1962) A new model for secondary nondisjunction: the role of distributive pairing. Genetics 47:1737

Haldane JBS (1919) The combination of linkage values and the calculation of distances between the loci of linked factors. J Genet 8:299–309

Hammer MF, Schimenti J, Silver LM (1989) Evolution of mouse chromosome 17 and the origin of inversions associated with t haplotypes. Proc Natl Acad Sci 86:3261–3265

Hatkevich T, Kohl KP, McMahan S, Hartmann MA, Williams AM, Sekelsky J (2017) Bloom syndrome helicase promotes meiotic crossover patterning and homolog disjunction. Curr Biol 27:96–102

Hilliker AJ, Harauz G, Reaume AG, Gray M, Clark SH, Chovnick A (1994) Meiotic gene conversion tract length distribution within the rosy locus of *Drosophila melanogaster*. Genetics 137:1019–1026

Housworth EA, Stahl FW (2003) Crossover interference in humans. Am J Hum Genet 73:188–197

Hughes SE, Miller DE, Miller AL, Hawley RS (2018) Female meiosis: synapsis, recombination, and segregation in *Drosophila melanogaster*. Genetics 208:875–908

Kleckner N, Zickler D, Jones GH, Dekker J, Padmore R, Henle J et al. (2004) A mechanical basis for chromosome function. Proc Natl Acad Sci 101:12592

Kosambi DD (1943) The estimation of map distance from recombination values. Ann Eugen 12:172–175

Lucchesi JC, Suzuki DT (1968) The interchromosomal control of recombination. Annu Rev Genet 2:53–86

Mackay TFC, Richards S, Stone EA, Barbadilla A, Ayroles JF, Zhu D et al. (2012) The *Drosophila melanogaster* genetic reference panel. Nature 482:173–178

Martini E, Diaz RL, Hunter N, Keeney S (2006) Crossover homeostasis in yeast meiosis. Cell 126:285–295

McPeek MS, Speed TP (1995) Modeling interference in genetic recombination. Genetics 139:1031–1044

Miller DE, Cook KR, Arvanitakis AV, Hawley RS (2016a) Third chromosome balancer inversions disrupt protein-coding genes and influence distal recombination events in *Drosophila melanogaster*. *G3*. Genes, Genomes, Genet 6:1959–1967

Miller DE, Cook KR, Kazemi NY, Smith CB, Cockrell AJ, Hawley RS et al. (2016b) Rare recombination events generate sequence diversity among balancer chromosomes in *Drosophila melanogaster*. Proc Natl Acad Sci 113:E1352–E1361

Miller DE, Smith CB, Kazemi NY, Cockrell AJ, Arvanitakis AV, Blumenstiel JP et al. (2016c) Whole-genome analysis of individual meiotic events in *Drosophila melanogaster* reveals that noncrossover gene conversions are insensitive to interference and the centromere effect. Genetics 203:159–171

Miller DE, Cook KR, Hemenway EA, Fang V, Miller AL, Hales KG et al. (2018) The molecular and genetic characterization of second chromosome balancers in *Drosophila melanogaster*. G3 Genes, Genomes, Genet 8:1161–1171

Morgan C, Fozard JA, Hartley M, Henderson IR, Bomblies K, Howard M (2021) Diffusion-mediated HEI10 coarsening can explain meiotic crossover positioning in Arabidopsis. Nat Commun 12:1–11

Morgan TH, Bridges CB, Schultz J (1935) Report of investigations on the constitution of the germinal material in relation to heredity. Pub Carnegie Instn Washing 34:284–291

Morgan TH, Bridges CB, Sturtevant AH (1925) The genetics of Drosophila. Biblio Gen 2:1–262

Muller HJ (1916) The mechanism of crossing-over. II. IV. The manner of occurrence of crossing-over. Am Nat 50:284–305

Navarro A, Betrán E, Barbadilla A, Ruiz A (1997) Recombination and gene flux caused by gene conversion and crossing over in inversion heterokaryotypes. Genetics 146:695–709

Novitski E, Braver G (1954) An analysis of crossing over within a heterozygous inversion in *Drosophila melanogaster*. Genetics 39:197

Otto SP, Payseur BA (2019) Crossover interference: shedding light on the evolution of recombination. Annu Rev Genet 53:19–44

Owen ARG (1949) The theory of genetical recombination. I. Long-chromosome arms. Proc R Soc Lond Ser B-Biol Sci 136:67–94

Page SL, Hawley RS (2001) *c(3)G* encodes a Drosophila synaptonemal complex protein. Genes Dev 15:3130–3143

Page SL, Hawley RS (2004) The genetics and molecular biology of the synaptonemal complex. Annu Rev Cell Dev Biol 20:525–558

Parker JS (1987) Increased chiasma frequency as a result of chromosome rearrangement. Heredity 58:87–94

Payne LC (1956) The theory of genetical recombination: a general formulation for a certain class of intercept length distributions appropriate to the discussion of multiple linkage. Proc R Soc Lond Ser B-Biol Sci 144:528–544

Pazhayam NM, Turcotte CA, Sekelsky J (2021) Meiotic crossover patterning. Front Cell Dev Biol 9:1940

Ramel C (1968) The effect of the Curly inversions on meiosis in *Drosophila melanogaster*. Hereditas 60:211–222

Risch N, Lange K (1983) Statistical analysis of multilocus recombination. Biometrics 39:949–963

Roberts P (1962) Interchromosomal effects and the relation between crossing-over and nondisjunction. Genetics 47:1691

Roberts PA (1967) A positive correlation between crossing over within heterozygous pericentric inversions and reduced egg hatch of Drosophila females. Genetics 56:179

Roberts PA (1972) Differences in synaptic affinity of chromosome arms of *Drosophila melanogaster* revealed by differential sensitivity to translocation heterozygosity. Genetics 71:401–415

Rog O, Köhler S, Dernburg AF (2017) The synaptonemal complex has liquid crystalline properties and spatially regulates meiotic recombination factors. Elife 6:e21455

Schultz J, Redfield H (1951) Interchromosomal effects on crossing over in Drosophila. Cold Spring Harb Symp Quant Biol 16: 175–197

Sidhu GK, Fang C, Olson MA, Falque M, Martin OC, Pawlowski WP (2015) Recombination patterns in maize reveal limits to crossover homeostasis. Proc Natl Acad Sci 112:15982–15987

Sinclair DA (1975) Crossing over between closely linked markers spanning the centromere of chromosome 3 in *Drosophila melanogaster*. Genet Res 26:173–185

Sokal RR, Rohlf FJ (1995) Biometry: the principles and practice of statistics in biological research. W.H. Freeman Company, New York

Stam P (1979) Interference in genetic crossing over and chromosome mapping. Genetics 92:573–594

Stauffer WT, Zhang L, Dernburg A (2019) Diffusion through a liquid crystalline compartment regulates meiotic recombination. In: *Biophysics, biology and biophotonics IV: the crossroads*, International Society for Optics and Photonics Vol 10888, p 1088809

Stenløkk K, Saitou M, Rud-Johansen L, Nome T, Moser M, Árnyasi M et al. (2022) The emergence of supergenes from inversions in Atlantic salmon. Philos Trans R Soc B 377:20210195

Stevens WL (1936) The analysis of interference. J Genet 32:51–64

Stevison LS, Hoehn KB, Noor MAF (2011) Effects of inversions on within-and between-species recombination and divergence. Genome Biol Evol 3:830–841

Stone W, Thomas I (1935) Crossover and disjunctional properties of *X* chromosome inversions in *Drosophila melanogaster*. Genetica 17:170–184

Sturtevant AH (1913) The linear arrangement of six sex linked factors in Drosophila, as shown by their mode of association. J Exp Zool 14:43–59

Sturtevant AH (1915) The behavior of the chromosomes as studied through linkage. Z Indukt Abstamm-und Vererb 13:234–287

Sturtevant AH (1917) Genetic factors affecting the strength of linkage in Drosophila. Proc Natl Acad Sci 3:555

Sturtevant AH (1921) A case of rearrangement of genes in Drosophila. Proc Natl Acad Sci 7:235

Sturtevant AH, Beadle GW (1936) The relations of inversions in the *X* chromosome of *Drosophila melanogaster* to crossing over and disjunction. Genetics 21:554–604

Termolino P, Falque M, Aiese Cigliano R, Cremona G, Paparo R, Ederveen A et al. (2019) Recombination suppression in heterozygotes for a pericentric inversion induces the interchromosomal effect on crossovers in Arabidopsis. Plant J 100:1163–1175

Thomas JW, Cáceres M, Lowman JJ, Morehouse CB, Short ME, Baldwin EL et al. (2008) The chromosomal polymorphism linked to variation in social behavior in the white-throated sparrow (*Zonotrichia albicollis*) is a complex rearrangement and suppressor of recombination. Genetics 179:1455–1468

Wang S, Zickler D, Kleckner N, Zhang L (2015) Meiotic crossover patterns: obligatory crossover, interference and homeostasis in a single process. Cell Cycle 14:305–314

Weinstein A (1918) Coincidence of crossing over in *Drosophila melanogaster* (*Ampelophila*). Genetics 3:135

Weinstein A (1936) The theory of multiple-strand crossing over. Genetics 21:155

Zetka M-C, Rose AM (1992) The meiotic behavior of an inversion in *Caenorhabditis elegans*. Genetics 131:321–332

Zhang L, Köhler S, Rillo-Bohn R, Dernburg AF (2018) A compartmentalized signaling network mediates crossover control in meiosis. Elife 7:e30789

Zhang L, Liang Z, Hutchinson J, Kleckner N (2014) Crossover patterning by the beam-film model: analysis and implications. PLoS Genet 10:e1004042

Zhang L, Wang S, Yin S, Hong S, Kim KP, Kleckner N (2014) Topoisomerase II mediates meiotic crossover interference. Nature 511:551–556

Zhao H, Speed TP, McPeek MS (1995) Statistical analysis of crossover interference using the chi-square model. Genetics 139:1045–1056

ACKNOWLEDGEMENTS

This work was conducted in partial fulfillment of the author's Ph.D. dissertation at Stony Brook University supported by NIH Project #1 R01 GM090094 awarded to Walt Eanes, the author's dissertation advisor. The author wishes to thank Walt Eanes, Josh Rest, John True, and Elise Lauterbur of Stony Brook University, David Rand of Brown University, Rob Unckless and Justin Blumenstiel of University of Kansas, Scott Hawley and Sarah Zanders of Stowers Institute for Medical Research for providing advice and helpful insights in the preparation of this manuscript for publication.

AUTHOR CONTRIBUTIONS

SAK was responsible for conception, design, execution, analysis, and interpretation of all experiments in this study. SAK conducted the modeling and prepared the manuscript for publication.

COMPETING INTERESTS

The author declares no competing interests.

ADDITIONAL INFORMATION

Supplementary information The online version contains supplementary material available at https://doi.org/10.1038/s41437-023-00593-x.

Correspondence and requests for materials should be addressed to Spencer A. Koury.

Reprints and permission information is available at http://www.nature.com/reprints

Publisher's note Springer Nature remains neutral with regard to jurisdictional claims in published maps and institutional affiliations.